CORTEX 194 (2026) 35–49

Available online at www.sciencedirect.com

ScienceDirect

Journal homepage: www.elsevier.com/locate/cortex

Research Report

Beta-band modulation reveals the cortical dynamics of auditory statistical learning in children

Jarrad A.G. Lum [a,*], Christine N. Moreau [b], Li-Ann Leow [c,d], Welber Marinovic [e], Sarah J. Lum [f], Marc F. Joanisse [b] and Laura J. Batterink [b]

[a] Cognitive Neuroscience Unit, School of Psychology, Deakin University, Australia
[b] Department of Psychology, Centre for Brain and Mind, Western University, London, Canada
[c] School of Psychology, The University of Queensland, Australia
[d] School of Arts and Humanities, Edith Cowan University, Australia
[e] Curtin School of Population Health, Curtin University, Australia
[f] Department of Endocrinology, Monash Health, Australia

ARTICLE INFO

Article history:
Received 26 June 2025
Revised 5 November 2025
Accepted 5 November 2025
Action editor Richard J. Binney
Published online 15 November 2025

Keywords:
Auditory statistical learning
Neural oscillations
Electroencephalography
Beta oscillations

ABSTRACT

Children's ability to extract statistical regularities from speech is considered fundamental to lexical, syntactic, and grammatical development. However, the neural oscillatory mechanisms supporting this process in childhood remains poorly understood. While beta-band oscillations have been linked to statistical learning in visual and motor domains, it is unclear whether similar dynamics support auditory statistical learning in children. In this study, we recorded electroencephalography (EEG) from children aged 8–12 years as they listened to a continuous stream of trisyllabic nonwords (e.g., dapiku), where syllable order within each nonword was fixed (high predictability), but transitions between nonwords were variable (low predictability). Beta power was significantly lower for the more predictable second and third syllables relative to the less predictable first syllable. This effect emerged only after repeated exposure and was localised to left prefrontal electrodes. Beta power also correlated with post-exposure recognition accuracy. Additional learning-related modulations were observed in the theta-alpha and delta-theta bands, suggesting broader oscillatory engagement. These findings indicate that auditory statistical learning in middle childhood engages frequency-specific neural dynamics, with beta power modulations showing parallel effects to those observed in other modalities.

* *Corresponding author*. School of Psychology, Deakin University, 221 Burwood Highway, Burwood, Victoria, 3125, Australia.
E-mail address: jarrad.lum@deakin.edu.au (J.A.G. Lum).

https://doi.org/10.1016/j.cortex.2025.11.003

1. Introduction

Statistical learning describes the process of detecting regularities or patterns in sensory input (Romberg & Saffran, 2010). Often, this occurs incidentally or implicitly, as dependencies between elements in the environment are discovered without explicit instruction or conscious awareness (Aslin, 2017). For instance, infants, children, and adults become sensitive to high-probability syllable co-occurrences when passively listening to continuous speech (e.g., Batterink, 2017; Raviv & Arnon, 2018; Saffran, Aslin, & Newport, 1996). During childhood, this learning mechanism likely supports language development, for example, by facilitating word segmentation and contributing to the acquisition of grammatical and syntactic structures (Gómez & Gerken, 2000; Kidd, 2012; Kuhl et al., 2006; Ren et al., 2023; Saffran & Wilson, 2003; Wonnacott et al., 2008). At present, however, the neural basis of auditory statistical learning remains poorly understood (Batterink et al., 2019). The current study addressed this gap by examining the neural oscillatory dynamics underlying auditory statistical learning in children.

2. Neuroimaging studies of auditory linguistic statistical learning

To date, only a handful of studies have examined the neural basis of statistical learning for linguistic information in typically developing children (Fan et al., 2024; Finn et al., 2019; McNealy et al., 2010, 2011; Moreau et al., 2022). These studies commonly employ artificial speech segmentation paradigms (e.g., Saffran, Newport, & Aslin, 1996; Saffran et al., 1997), in which children are exposed to a continuous stream of syllables composed of three or four nonwords (e.g., dapiku, golatu, tibudo). During exposure, these nonwords are concatenated without pauses (e.g., dapikugolatutibudo), creating a hidden statistical structure that learners extract simply through exposure. Within a word, transitional probabilities between syllables are high (e.g., *da* predicts *pi* with 100% probability), whereas at word boundaries, syllable transitions are less predictable (e.g., *ku* may be followed by *go* or *ti* with equal probability). fMRI studies (McNealy et al., 2006, 2010, 2011) suggest that in young children (around 5–6 years old), listening to a continuous speech stream elicits bilateral activation in the frontal and temporal lobes. However, from 10 years of age into adulthood, this activity becomes increasingly left-lateralised (McNealy et al., 2011).

Children's sensitivity to statistical structure has also been linked to brain morphology. In the auditory statistical learning literature, nonword learning is typically assessed offline using a two-alternative forced-choice (2AFC) recognition task (e.g., Saffran et al., 1997). In this test, children hear one of the previously presented nonwords (e.g., dapiku) alongside a foil (e.g., latudo), which is composed of recombined syllables, and are asked to indicate which sounds more familiar. Behavioural studies consistently show that both children and adults perform above chance on this task after exposure (Isbilen & Christiansen, 2022; Saffran et al., 1997). Finn et al. (2019) demonstrated that, in 5–6-year-old children, superior recognition of nonwords correlated with cortical thickness in the left inferior prefrontal cortex and volume of the right hippocampus. This finding suggests that explicit recognition of the nonwords, post exposure, may recruit additional brain structures beyond the canonical left-lateralised language network.

3. Beta oscillations and statistical learning

Cycles of synchronised and desynchronised neural activity form the basis of information processing and transfer in the brain (Buzsaki & Draguhn, 2004). This oscillatory activity arises from the coordinated firing of cortical pyramidal neurons, generating rhythmic fluctuations that can be detected at the scalp using EEG and magnetoencephalography (MEG) (Cohen, 2017). In the human brain, neuronal populations synchronise at distinct frequency bands termed delta (1–4 Hz), theta (4–7 Hz), alpha (7–12 Hz), beta (12–30 Hz), and gamma (>30 Hz) (Buzsaki & Draguhn, 2004).

In M/EEG research, oscillatory activity within each frequency band is typically quantified as spectral power, defined as the squared amplitude of the signal. Power reflects the strength of rhythmic fluctuations recorded at the scalp, which can increase either because more neurons become temporally aligned (greater synchrony) or because individual neural populations oscillate with larger amplitude. Thus, while power and synchrony are related, they are not equivalent. Early work often interpreted increases in power as greater synchronisation (Pfurtscheller & Aranibar, 1977), but subsequent studies have demonstrated that power and synchrony are distinct neurophysiological properties. For example, Musall et al. (2014) showed that increases in EEG power can arise from greater synchrony even when local field potential amplitude decreases, and conversely, power can also increase purely through amplitude modulation without changes in synchrony. In this study, we therefore interpret event-related (de)synchronisation as relative changes in spectral power, without assuming they directly index underlying neural synchrony.

To our knowledge, no study has examined the oscillatory dynamics associated with auditory linguistic statistical learning in children. We suspect, however, oscillatory activity in the beta band may be sensitive to transitional probabilities in this group during auditory linguistic statistical learning. In adults, during statistical learning, beta power decreases following presentation of highly predictable stimuli relative to less predictable ones. Bogaerts et al. (2020) investigated this phenomenon using a visual statistical learning task that closely mirrored the auditory paradigm described above. In this study, adult participants were presented with a series of shapes, organised into hidden triplets, each appearing sequentially on a computer display. Within each triplet, the first shape reliably predicted the second and third, whereas the third shape had an equal probability of being followed by any shape from a different triplet. Thus, the transitional probabilities were high between consecutive shapes within a triplet, but low at triplet boundaries. Beta power was found to be significantly lower for the predictable shapes (e.g., Shape 2 and 3) compared to the less predictable shape (i.e., Shape 1).

This power difference was exposure dependent, with the difference in beta power between predictable and less predictable shapes only reaching statistical significance after repeated exposures to visual triplets. Furthermore, correlation analyses indicated that the difference in beta power for within-versus between-pattern transitions was associated with better identification of triplets in an offline 2AFC recognition test.

Beta activity also appears to be sensitive to stimulus probability or predictability in the motor domain in adults and children. In adults, Lum et al. (2024) found beta power declined as participants implicitly repeated a sequence of finger movements, before increasing at the end of the task when random finger movements were generated. This modulation in beta power was specific electrodes above motor areas. Furthermore, correlation analyses demonstrated that faster reaction times were associated with lower beta power. This result was replicated by Lum et al. (2025) in a sample of 10-year old children, who were similar in age to the children who participated in the present study. As in adults, children's beta power over the motor area decreased as they implicitly learnt a sequence of finger movements and then increased when random movements were made (Lum et al., 2025). Furthermore, beta-related sensitivity to sequenced finger movements was not present in a group of children with clinically significant motor difficulties, who failed to learn the motor sequence. Thus, there is growing evidence that reductions in beta power co-occur with predictable stimuli. The present study examined whether same oscillatory dynamics that underpin sensitivity to statistical structure in the motor and visual domains also extend to auditory linguistic learning .

Decreases in beta power, or beta desynchronisation, reflect active information processing in the brain (Pfurtscheller et al., 2003). This is well demonstrated in the motor domain, where finger or hand movements result in a decrease in beta power recorded over motor areas (Pfurtscheller, 1992). This reduction occurs because, as a neural assembly synchronises to execute a movement, it desynchronises from broader resting-state networks, leading to fewer neurons oscillating in the beta band and, consequently, lower beta power. However, once the movement is completed, the neural assembly re-synchronises with the broader resting-state network, resulting in a rebound increase in beta power (Pfurtscheller & Lopes da Silva, 1999). An influential model proposed by Engel and Fries (2010) suggests that beta desynchronisation (i.e., decreases in beta power relative to baseline) serves as a mechanism that enables incoming sensory information to reshape functional networks. In the context of statistical learning, beta desynchronisation on predictable stimuli may reflect the brain's active processing of the underlying statistical structure, facilitating the updating of neural representations as patterns are extracted from the sensory input. Some accounts of statistical learning, suggest that children may rely more heavily on these bottom-up mechanisms than adults (Berger & Batterink, 2024; Janacsek et al., 2012), potentially making oscillatory markers of sensory-based learning more salient in childhood.

Further supporting the role of beta oscillations in auditory statistical learning, other research has demonstrated that beta-band activity is sensitive to temporal regularities in auditory sequences. Fujioka et al. (2012) found that beta oscillations in the auditory cortex and motor-related areas track the predictive timing of isochronous sound sequences, even during passive listening without movement. In their study, beta power decreased immediately after stimulus onset but then rebounded to peak just before the next expected sound, with the timing of this rebound scaling with stimulus rate only during regular sequences. This suggests that beta oscillations may also provide a neural mechanism for maintaining predictive timing information about when the next auditory event is expected. Additionally, research has shown that beta-band modulations are linked to temporal prediction in tone sequences and tone pitch prediction (Chang et al., 2018).

4. Study aim and hypotheses

This study investigated neural oscillatory activity during auditory statistical learning in children aged around 10 years of age. In the study, children listened to an artificial speech stream composed of randomly presented tri-syllabic nonwords while EEG was continuously recorded. Based on findings from statistical and sequence learning in visual and motor domains (Bogaerts et al., 2020; Lum et al., 2024, 2025), we hypothesised that beta power would be lower for the highly predictable second and third syllable, compared to the less predictable first syllable. We further hypothesised that this difference would emerge only after repeated exposure to the nonwords, as statistical learning depends on the accumulation of transitional probability information over time. We also expected learning-related beta activity to be left-lateralised given the stimuli were speech sounds. This prediction was based on evidence that beta oscillations occur within modality specific networks; they have been linked to occipital regions during visuospatial processing (Kloosterman et al., 2015), motor cortex during movement (Pfurtscheller & Lopes da Silva, 1999), and left-hemisphere regions during language processing (Weiss & Mueller, 2012). Finally, we hypothesised that greater desynchronisation in the beta band to predictable syllables would be associated with better performance on an offline measure of statistical learning, thereby replicating findings from visual and motor domains (Bogaerts et al., 2020; Lum et al., 2024, 2025).

5. Method

5.1. *Participants*

This study re-analysed paediatric EEG and behavioural data from an auditory statistical learning study undertaken by Moreau et al. (2022), with the raw data accessed via Mendeley Data (Moreau, 2022). A total of 56 children (24 females) aged between 8 and 12 years participated in the study ($M = 9.98$ years; $SD = 1.26$ years). Children's receptive grammatical skills were assessed using the Test for Reception of Grammar-2 (Bishop, 2003). Performance on the test is described by a standardised score (i.e., mean of 100 and standard deviation of 15). The mean standard score for the sample was 105.2 ($SD = 10.9$). All children spoke English as

their first language. Families participating in the study were recruited from London, Ontario. Informed written consent was obtained from the parents, and assent was obtained from the children.

5.2. Materials

Auditory Statistical Learning Paradigm. Children completed an auditory statistical learning paradigm modified from Batterink and Paller (2017). This paradigm comprises two phases: an exposure phase that involves presenting a continuous auditory stream composed of four repeating trisyllabic nonwords, followed by a test phase, which includes a 2AFC recognition task to assess the extent the nonwords were learnt.

The auditory stimuli presented to the children for the exposure period were four nonwords: 'pautone', 'nurafi', 'gabalu', and 'mailoki'. The nonwords were concatenated into a continuous stream without any pauses between words, presented in pseudo-random order, with the only constraint that the same nonword could not be presented consecutively. Importantly, since randomisation occurred at the nonword, but not syllabic level, the transitional probability between syllables within a nonwords was 1.0, but between nonwords, .33. For example, if the syllable 'ga' was presented, there was a 100% probability the next syllable would be 'ba' and the following syllable 'lu' (as in 'ga-ba-lu'). However, if the syllable 'lu' was presented, there was 33% probability the next syllable would be either 'pa' (as in pa-utone), 'nu' (as in nu-rafi) or 'ma' (as in 'mai-loki'). The nonwords were presented to the children at a rate of one syllable every 300 msec; thus each word was presented at a rate of 1.1 Hz and each syllable, 3.3 Hz. Each nonword was presented 100 times, for a total of 400-word presentations and yielding a stream duration of 6 min. As children listened to the auditory stimuli they watched 'Shaun the Sheep', with no audio, to reduce boredom and movement.

After the exposure period, children were presented with a series of tasks that assessed their ability to recognise the four nonwords previously presented. This included a familiarity rating task, target detection task and 2AFC recognition task (for details see Moreau, 2022). On the familiarity rating task, participants rated the familiarity of items on a 1–4 scale, including words, partword foils, and nonword foils. On the target detection task, participants responded as quickly as possible to target syllables within structured speech streams, providing a reaction time-based measure of statistical learning. In the current study we focused on data from the 2AFC recognition task, which tests explicit knowledge of the nonwords and is a widely used index of statistical learning in this literature (Isbilen & Christiansen, 2022). This task has also been previously used to examine the association between beta activity and statistical learning in the visual domain (Bogaerts et al., 2020). On this task children are presented with the nonwords from the exposure period (e.g., 'pautone', 'nurafi', 'gabalu', and 'mailoki') along with foils. Two types of foils were presented, one by randomly selecting three syllables (e.g., ki-pau-to) to create a nonword not previously heard, and the other, by randomly replacing a single syllable from the target nonwords to create a partially familiar word (e.g., nu-ba-lu). The 2AFC task consisted of 16 trials, created by pairing each nonword and foil. On each trial the nonword and foil were presented one at a time, separated by a 1500 msec pause. Presentation order of the nonword and foil on each trial was randomised. For each trial, children were asked to indicate whether the first or second item was more familiar. Performance on this task was described in terms of the proportion of correct responses.

5.3. EEG data acquisition & pre-processing

EEG was continuously acquired during the 6-min exposure period using a Biosemi Active-Two system with 32 Ag/AgCl electrodes embedded in an elastic cap. Electrodes were positioned according to the 10–10 EEG system, and data were sampled at 512 Hz with a Common Mode Sense reference. Event markers were inserted to mark the onset of each syllable.

Pre-processing was performed in MATLAB (Version 2024b) using EEGLAB (Version 2024.2.1; Delorme & Makeig, 2004) and the RELAX toolbox (Bailey et al., 2023a, 2023b). The following pre-processing steps were applied in sequence:

1. Down-sampling: Raw EEG was down-sampled from 512 Hz to 250 Hz to reduce computational demands.
2. Re-referencing: Data were initially re-referenced to the common average. This step improves the independent component decomposition used in Step 4, by distributing variance more evenly across channels, reducing the likelihood that multiple artifact sources load onto the same component. After artifact correction, the data were re-referenced to the average of the left and right mastoids, which served as the final reference for all analyses.
3. Filtering: A .25–80 Hz band-pass filter was applied.
4. Artifact correction:
   - Oculomotor, line noise, muscle, and other artifacts were reduced using Multiple Wiener Filtering.
   - Residual artifacts were further addressed with wavelet-enhanced Independent Component Analysis (Castellanos & Makarov, 2006) combined with ICLabel classification (Pion-Tonachini et al., 2019).
5. Noisy channel handling: Noisy channels were automatically detected using the findNoisyChannels function from the PREP pipeline (Bigdely-Shamlo et al., 2015). Electrodes were flagged if they exceeded thresholds for absolute voltage shift (500 μV), improbable voltage distributions (kurtosis >8 at the channel or global level), or median absolute deviation (20). Flagged channels were subsequently interpolated.
6. Artifact correction was performed with FastICA combined with wavelet-enhanced ICA (wICA), and components were classified using ICLabel with no visual inspection.
7. Re-referencing: After cleaning, data were re-referenced to the average of the left and right mastoids.
8. Channel exclusion: Electrodes used to capture ocular activity were excluded from further analyses.
9. Epoching: Continuous EEG was segmented into epochs from −1000 msec to 2000 msec relative to the onset of the first syllable of each nonword. Although analyses focused on oscillatory activity during individual syllables (300 msec) and nonwords (900 msec), extended epochs

were used to avoid edge artifacts during time–frequency decomposition.

After pre-processing, the average number of epochs per child submitted to time-frequency decomposition, out of a maximum of 400, was 360 ($SD = 19$; Range: 312, 387).

5.4. Time-frequency analysis

Complex Morlet wavelets were used to derive oscillatory power over time and frequency from the time-series voltage data. The wavelets were defined as $e^{i2\pi ft}e^{-t^2/(2\sigma^2)}$, with frequency values (f) ranging from 1 to 35 Hz in 100 linearly spaced steps. The wavelet width ($\sigma = n/[2\pi f]$), defined in cycles n, ranged from 3 to 15 logarithmically spaced steps. These parameters provided optimal temporal and frequency resolution across the frequency and time ranges of interest. Time–frequency decomposition was performed separately for each trial, electrode, and frequency. The result of the time frequency analysis was oscillatory activity measured in terms of power (μV^2), computed separately for each trial, electrode, frequencies and each time point in the epoch. Power values (μV^2) were then averaged across trials for each nonword type to yield condition-level estimates. After averaging, the data were trimmed to match the length of a single nonword (0–900 msec, relative to onset of the first syllable). The trimmed data were then decibel (dB) baseline-corrected relative to the mean power of the entire nonword window (0–900 msec). In a final step, baseline-corrected time–frequency data were down-sampled to 50 Hz. This reduced computational load while preserving temporal resolution (Cohen, 2014). For illustrative purposes, Fig. 1 shows down-sampled, dB-corrected time–frequency data averaged across trials, electrodes, and participants. Time zero marks the onset of the first syllable, and vertical lines at 300 and 600 msec indicate the second and third syllable onsets. Time–frequency analyses were undertaken in MATLAB using scripts adapted from Cohen (2014).

5.5. Data analysis and permutation testing

Two sets of analyses were conducted. The first examined whether the predictability of syllables modulated oscillatory power. Based on previous research (Bogaerts et al., 2020; Lum et al., 2024), we hypothesised that highly predictable syllables (i.e., 2nd & 3rd syllables) would be associated with lower beta power compared to the less predictable syllable (i.e., 1st syllable). To test this, oscillatory power differences were examined in three contrasts:

- 1st syllable versus 3rd syllable
- 1st syllable versus 2nd syllable
- 2nd syllable versus 3rd syllable

These comparisons were conducted across all electrodes ($n = 30$), frequencies ranging from 1 to 35 Hz ($n = 100$), and time points ($n = 16$; 0–300 msec at a sampling rate of 50 Hz). This resulted in 4800 univariate tests per contrast. To control for multiple comparisons, permutation testing with cluster correction (Cohen, 2014; Maris & Oostenveld, 2007; Nichols & Holmes, 2002) was applied. This approach allows for thousands of univariate tests to be undertaken while maintaining alpha at .05.

Permutation testing was used to generate an empirical null distribution under the assumption that no reliable difference in oscillatory power existed between the syllable contrast at any electrode, frequency, or time point. This was achieved by randomly shuffling syllable labels within participants. For example, when testing the 1st syllable versus 3rd syllable contrast, the label for the 1st syllable could be randomly assigned to data originally associated with the 3rd syllable, and vice versa. For each permutation, t-values were computed

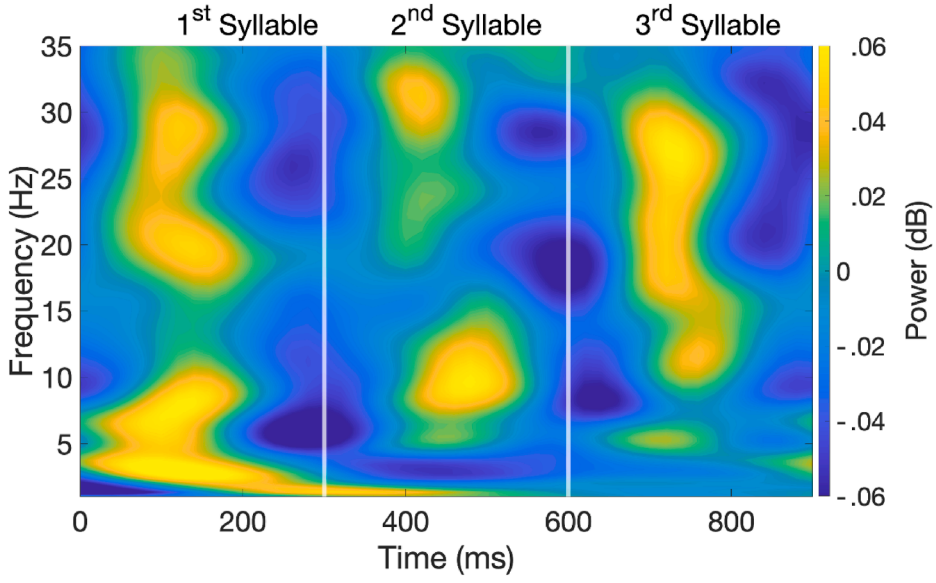

Fig. 1 – Time-frequency plot showing baseline dB correct power averaged over scalp electrodes, participants and trials. In this figure time zero indicates nonword onset and the white vertical lines indicate second and third syllable onsets.

for every time-frequency point at each electrode, generating a *t*-statistic matrix. A threshold of $\alpha = .05$ (two-tailed) was applied to identify significant clusters, defined as at least two adjacent significant time-frequency data points. The size of the largest observed cluster across all electrodes was recorded and stored as a single data point in the empirical null distribution. This process of shuffling syllable labels, calculating *t*-values, applying significance thresholds, and recording the largest cluster size was repeated 10,000 times, producing an empirical null distribution of expected cluster sizes under the null hypothesis. In the original (non-permuted) dataset, *t*-values were computed in the same manner, and significant clusters were identified by thresholding the time-frequency matrices across all electrodes. A cluster was deemed statistically significant in the original (non-permuted) data if its size exceeded the 95th percentile of the empirical null distribution ($p < .05$; nb: This step necessarily involves a one-tailed test, as the null distribution defines the maximum cluster sizes expected by chance; testing for unusually small clusters would not be meaningful, since small clusters are an inevitable outcome of noise.). Our approach to define clusters based on size, rather than, the sum of *t*-values, was selected to ensure analytic methods were comparable with our past research which demonstrated statistical/sequence learning in the motor domain modulated beta oscillations (Lum et al., 2024, 2025). Moreover, evidence from simulation studies show that defining clusters in terms of size or sum of *t*-values is associated with equivalent Type I error rates (Pernet et al., 2015).

The second set of analyses examined the relationship between auditory statistical learning performance, as measured by the two-alternative forced-choice (2AFC) recognition task, and oscillatory power during the exposure phase of the learning task. Based on previous research (Bogaerts et al., 2020; Lum et al., 2024, 2025), we hypothesised that lower beta power during exposure would be associated with higher 2AFC recognition scores. To test this, permutation testing with cluster correction was used to assess the reliability of the correlation between 2AFC scores and oscillatory power across all electrodes, frequencies, and time points.

The procedure first involved randomly shuffling 2AFC recognition scores across participants and then computing Spearman's ρ between the shuffled 2AFC scores and oscillatory power at each time-frequency data point, generating a ρ-statistic matrix for each electrode. Significance for each ρ value was determined using a threshold of $\alpha = .05$ (two-tailed), with clusters defined as at least two adjacent significant ρ-values. The size of the largest cluster from each permutation was recorded to construct an empirical null distribution, representing the largest clusters expected by chance across all electrodes, frequencies, and time points under the null hypothesis. This process of shuffling 2AFC scores, computing ρ-values, thresholding significant clusters, and extracting the largest cluster size was repeated 10,000 times to generate the null distribution. For the original (non-permuted) dataset, Spearman's ρ was computed in the same manner, and significant clusters were identified by thresholding the time-frequency matrices across all electrodes. A cluster was deemed statistically significant if its size exceeded the 95th percentile of the empirical null distribution ($p < .05$). Permutation testing was implemented using modified scripts based on Cohen (2014).

5.6. *Open science statement*

All data files used in this study along with MATLAB scripts necessary to replicate the analyses and figures presented in the results section can be found at the OSF site associated with this work (https://osf.io/e3ajh). The raw EEG, behavioural data and experiment stimuli can be accessed via Mendeley Data (Moreau, 2022).

6. Results

6.1. *Time-frequency analysis*

1st Syllable versus 3rd Syllable Contrast. Permutation analyses identified significant clusters at electrodes FC5 ($p = .009$) and T7 ($p = .040$; see Fig. S1 in Supplementary Materials for time–frequency *t*-maps for all electrodes and Fig. S2 for individual *t*-maps of FC5 & T7), which both showed higher power for the first syllable compared to the third. For visualisation and follow-up analyses, data from these two electrodes were averaged, given their spatial proximity and comparable modulations in oscillatory power. The cluster spanned frequencies between 18–27 Hz, indicative of beta band activity. The time–frequency *t*-map with data averaged across these electrodes is shown in Panel A of Fig. 2, with the significant cluster ($p = .002$) outlined by a white contour. As shown in Fig. 2, the strongest difference between syllables was localised to left prefrontal scalp regions.

For completeness, Panel B of Fig. 2 shows average power for the beta cluster at each syllable. This panel presents a swarm plot showing each child's average cluster power at each syllable. Pairwise comparisons using Wilcoxon Signed-Rank Tests with FDR-corrected *p*-values (Benjamini & Hochberg, 1995) confirmed the permutation findings: cluster power was lower for third syllable relative to the first ($p_{\text{FDR corrected}} = .003$). In addition, power at the 2nd syllable was significantly lower than at the 1st syllable ($p_{\text{FDR corrected}} = .013$), while the difference between 2nd and 3rd syllables was non-significant ($p_{\text{FDR corrected}} = .231$). Together, these analyses indicate that beta power was reduced for relatively more predictable syllables compared with less predictable ones.

In a further analysis, we tested whether the beta cluster from the previous analyses changed over the exposure period. For this analysis, average cluster power at the 1st and 3rd syllable was computed for each child within four sets of 100-trial epochs (i.e., trials 1–100, 101–200, 201–300, 301–400). Fig. 3 presents a swarm plot showing average power across these four epochs. Wilcoxon Signed-Rank Tests with FDR-corrected *p*-values indicated no significant difference in beta power between the 1st and 3rd syllables during the first 100 trials ($p_{\text{FDR corrected}} = .295$. However, from the second epoch onward, median power for the 3rd syllable was significantly lower compared to the 1st syllable (101–200: $p_{\text{FDR corrected}} = .003$; 201–300: $p_{\text{FDR corrected}} = .008$; 301–400: $p_{\text{FDR corrected}} = .001$).

1st Syllable versus 2nd Syllable Contrast. Permutation analyses revealed significant clusters spanning the theta–alpha

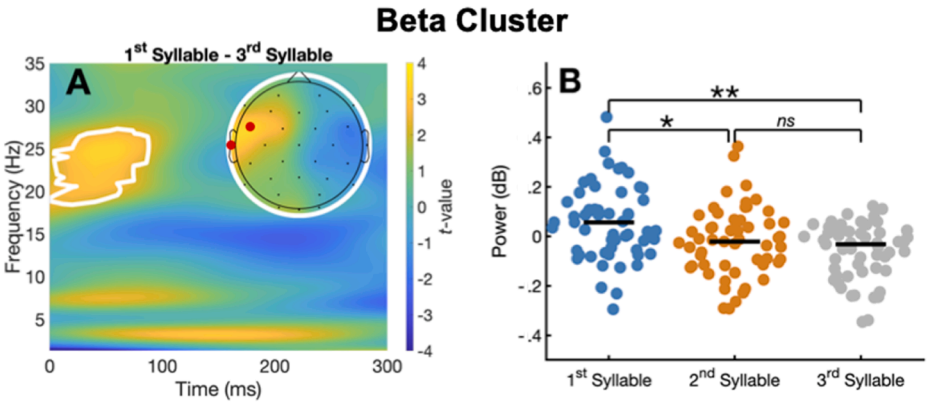

Fig. 2 – Panel A shows a time–frequency *t*-map of data averaged across electrodes FC5 and T7, with the significant beta cluster ($p = .002$) outlined in white. Lighter pixels (yellow) indicate greater power for the first syllable compared to the third, while darker pixels (blue) indicate the opposite. The inset displays the topographical distribution of power associated with the cluster, with FC5 and T7 highlighted in red. Panel B presents average cluster power for each child at each syllable. *$p < .001$; $p < .05$; *ns* = not significant, $p > .05$. All *p*'s FDR-corrected.

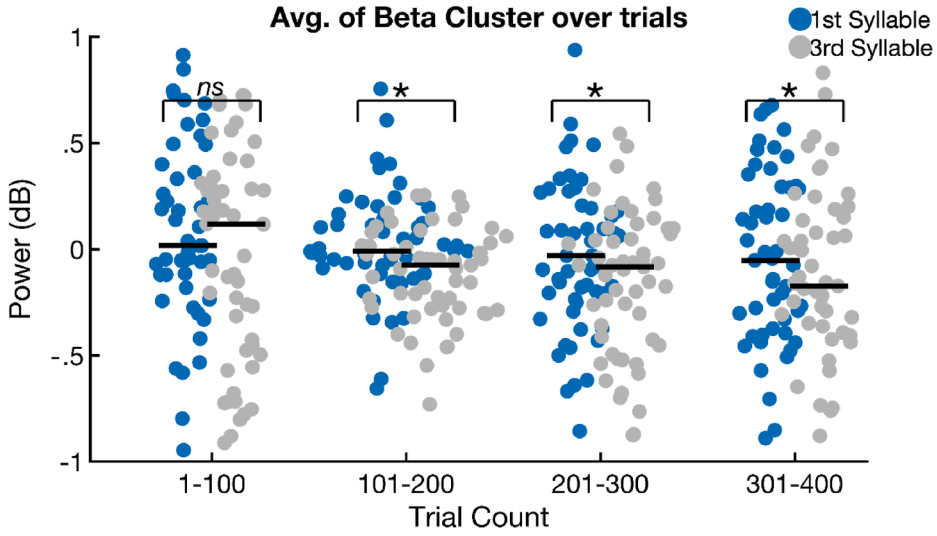

Fig. 3 – Swarm plot showing beta power (averaged across FC5 and T7 clusters) as a function of trial count epoch. Horizontal bars indicate median values. *$p < .05$; *ns* = not significant ($p > .05$). All *p*-values are FDR-corrected (two-tailed). Note that for the 1–100 trial epoch, the median difference between the first and third syllables appears visually large; however, the Wilcoxon Signed-Rank Test was nonsignificant because participants showed small or tied differences, reducing the overall ranked statistic despite the apparent separation in central tendency.

bands at frontal electrodes AF3 ($p = .017$), AF4 ($p = .040$), F3 ($p = .037$), Fz ($p = .022$), and FC5 ($p = .020$), in which power was higher at the second syllable compared to first. See Fig. S3 in Supplementary Materials for time–frequency *t*-maps for all electrodes from this contrast and Fig. S4 for individual *t*-maps of electrodes associated with significant clusters. Again, for visualisation and further analyses, data from these electrodes were averaged. Panel A of Fig. 4 presents the corresponding time–frequency *t*-map, with the significant cluster ($p = .003$) outlined in white. In this figure the frequency range of the cluster spanned 5–11 Hz, encompassing both theta and alpha bands. As shown in Fig. 4, differences in power between these syllables was largest at frontal scalp regions. To further characterise this effect, we examined average power of the theta-alpha cluster across syllables. Panel B of Fig. 4 presents a swarm plot of cluster power for each child at each syllable. Pairwise Wilcoxon Signed-Rank Tests with FDR-corrected *p*-values indicated that power significantly increased from the 1st to the 2nd syllable ($p_{\text{FDR corrected}} = .002$) and then plateaued, with the difference between the 2nd and 3rd syllables not significant ($p_{\text{FDR corrected}} = .113$). Power at the 3rd syllable was significantly higher compared to the 1st $p_{\text{FDR corrected}} = .006$).

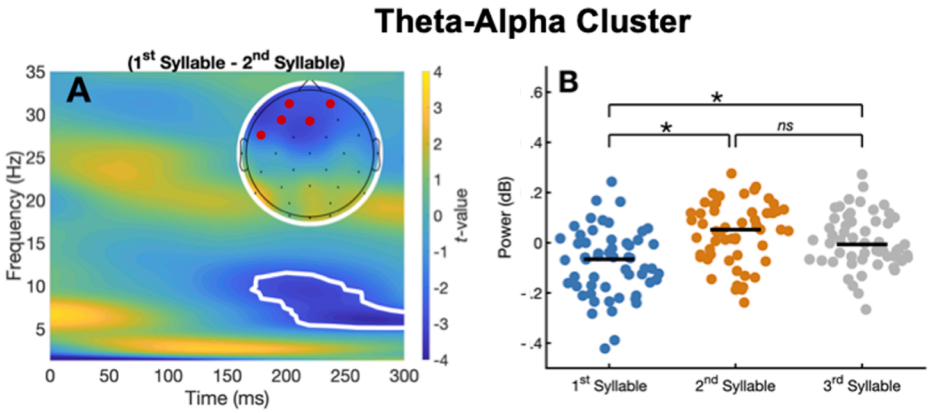

Fig. 4 – Panel A shows a time–frequency *t*-map of data averaged across electrodes AF3, AF4, F3, Fz and FC5, with the significant cluster ($p = .003$) outlined in white. Lighter pixels (yellow) indicate greater power for the first syllable compared to the third, while darker pixels (blue) indicate the opposite. The inset displays the topographical distribution of power associated with the cluster, with electrodes associated with significant clusters highlighted in red. Panel B presents average cluster power for each child at each syllable. *$p < .05$; *ns* = not significant, $p > .05$ (all *p*'s FDR-corrected).

Collectively, these analyses show that theta–alpha power was elevated at the more predictable syllables relative to the less predictable one.

Permutation analyses also revealed a second set of clusters spanning the delta–theta bands at central electrodes FC6 ($p = .030$), Cz ($p = .004$), and C4 ($p = .003$). See Fig. S5 for individual *t*-maps of electrodes associated with significant clusters. Panel A of Fig. 5 presents a time–frequency *t*-map from data averaged over these three electrodes, with the significant cluster outlined in white ($p = .001$). The frequency range of this cluster was 2–8 Hz which indicates delta-theta band activity. For this cluster, power was high on the second syllable compared to first. The inset shows the difference in power was concentrated over central regions of the scalp. Panel B of Fig. 5 shows average cluster power for each child at each syllable. Pairwise Wilcoxon Signed-Rank Tests with FDR-corrected *p*-values revealed that power significantly decreased from the 1st to the 2nd syllable ($p_{\text{FDR corrected}} < .001$) and from the 1st to 3rd syllable ($p_{\text{FDR corrected}} = .003$), while the difference between 2nd and 3rd syllables was not significant ($p_{\text{FDR corrected}} = .175$). Collectively, these results indicate that delta–theta power was reduced for the more predictable syllables relative to the less predictable one.

We also examined how the theta–alpha and delta–theta clusters changed over the course of exposure period. Specifically, we compared power differences between the 1st and 2nd syllables across four 100-trial epochs (i.e., trials 1–100, 101–200, 201–300, 301–400). Swarm plots and statistical results are shown in Fig. 6 (theta–alpha) and Fig. 7 (delta–theta). For the theta–alpha cluster, significant differences between

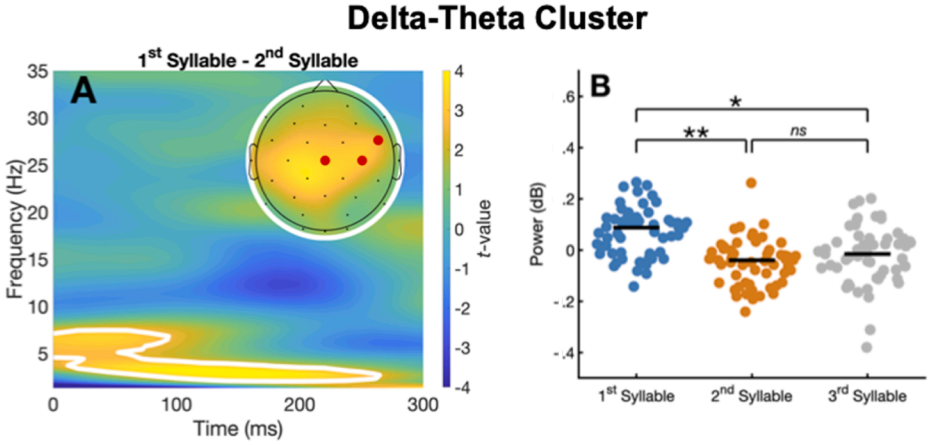

Fig. 5 – Panel A shows a time–frequency *t*-map of data averaged across electrodes FC6, Cz, and C4, with the significant cluster ($p = .001$) outlined in white. Lighter pixels (yellow) indicate greater power for the first syllable compared to the third, while darker pixels (blue) indicate the opposite. The inset displays the topographical distribution of power associated with the cluster, with electrodes associated with significant clusters highlighted in red. Panel B presents average cluster power for each child at each syllable. *$p < .001$; $p < .05$; *ns* = not significant, $p > .05$ (all *p*'s FDR-corrected).

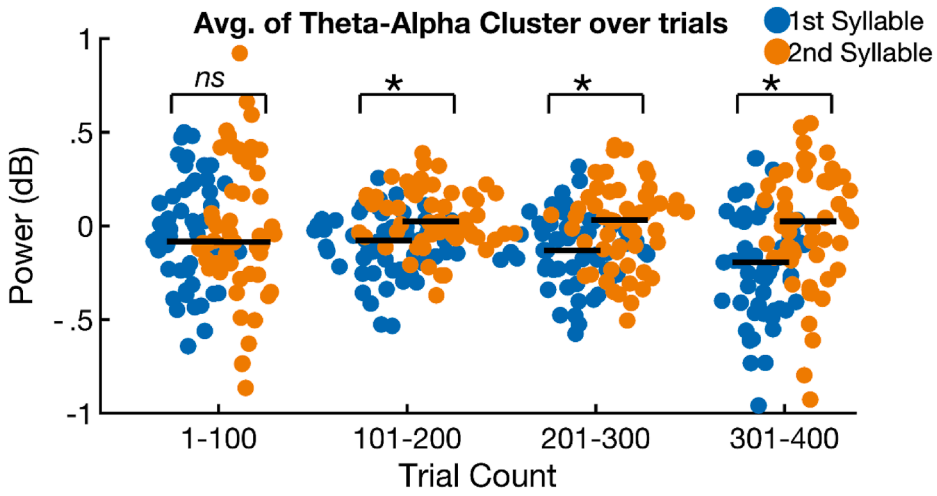

Fig. 6 – Differences in theta-power between the 1st and 2nd syllable across four 100-trial exposure epochs (trials 1–400). **$p < .001$; *$p < .05$; *ns* = not significant ($p > .05$). All *p*-values are FDR-corrected. In both panels, horizontal bars represent median values.

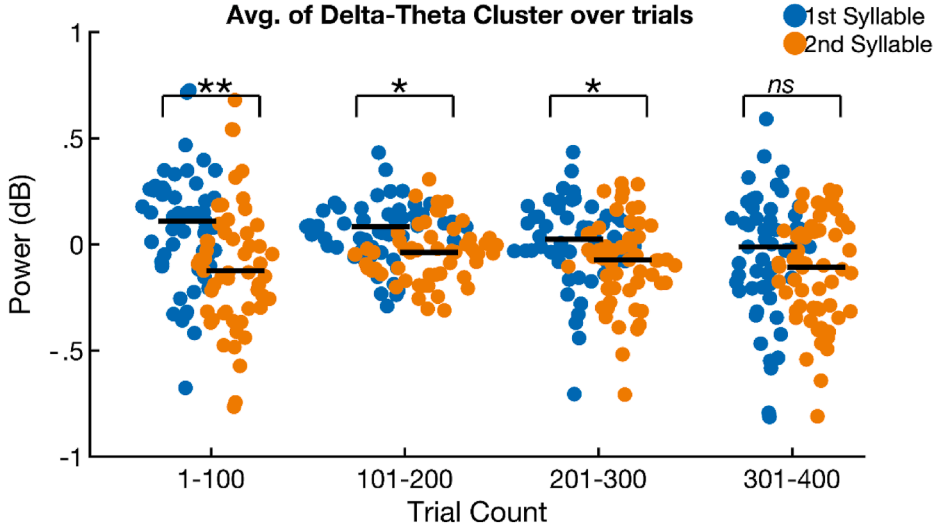

Fig. 7 – Differences in theta-power between the 1st and 2nd syllable across four 100-trial exposure epochs (trials 1–400). **$p < .001$; *$p < .05$; *ns* = not significant ($p > .05$). All *p*-values are FDR-corrected. In both panels, horizontal bars represent median values.

the 1st and 2nd syllables emerged from the second epoch onward (1–100: $p_{\text{FDR corrected}} = .586$; 101–200: $p_{\text{FDR corrected}} < .001$; 201–300: $p_{\text{FDR corrected}} = .003$; 301–400: $p_{\text{FDR corrected}} = .003$). At the delta–theta cluster, average power at the 1st syllable was significantly higher than the 2nd at all epochs (1–100: $p_{\text{FDR corrected}} < .001$; 101–200: $p_{\text{FDR corrected}} = .001$; 201–300: $p_{\text{FDR corrected}} = .002$) but the final epoch (301–400, $p_{\text{FDR corrected}} = .067$).

2nd Syllable versus 3rd Syllable Contrast. The final set of permutation tests examined differences in oscillatory power between the two highly predictable syllables. No significant clusters were identified in this analysis. Fig. S6 in the Supplementary Materials presents time-frequency *t*-maps for each electrode for this contrast.

6.2. *Correlation analysis*

The Relationship between the Offline Measure of Statistical Learning and Oscillatory Power. Finally, we conducted permutation-based correlation analyses to examine the relationship between oscillatory power and behavioural performance on the 2AFC recognition task. The behavioural data for this analysis consisted of accuracy scores previously reported by Moreau et al. (2022). On average, children responded correctly on

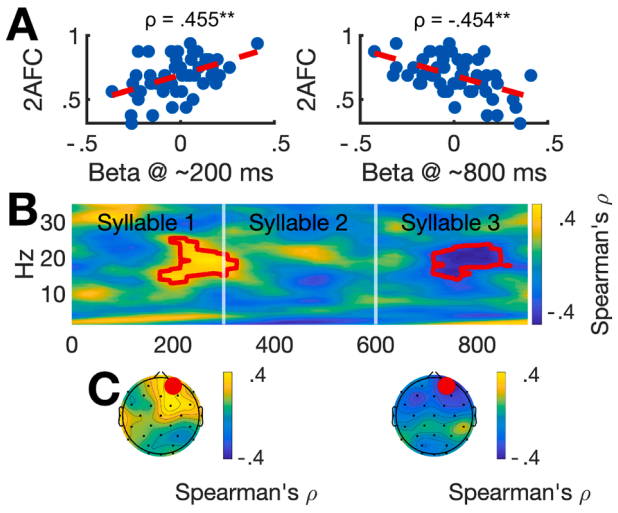

Fig. 8 – The relationship between oscillatory power and statistical learning at electrode AF4. The scatter plots in Panel A shows the association between beta power and 2AFC task accuracy at the two clusters (~200 msec & ~800 msec). Panel B shows the time-frequency correlation plot (Spearman's ρ) between oscillatory power and overall accuracy on the 2AFC task. In this panel, lighter colours (yellow) indicate positive correlations (Spearman's ρ) between accuracy and oscillatory power, while darker colours (blue) indicate negative correlations. Panel C shows the distribution of Spearman's ρ values across the scalp at each significant cluster. **$p < .001$

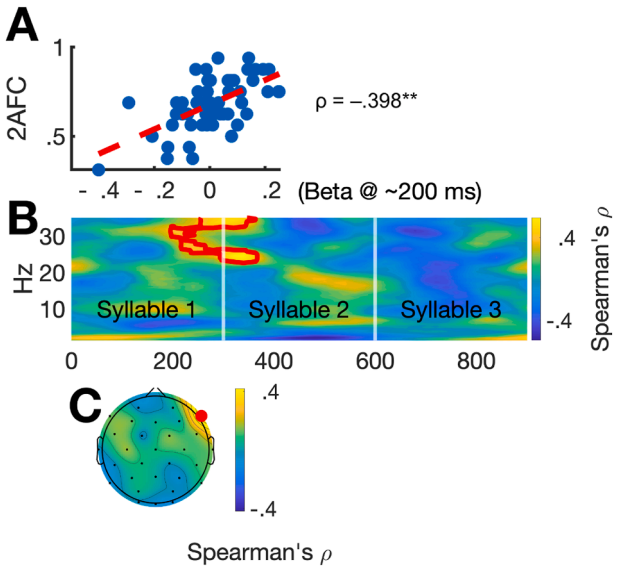

Fig. 9 – The relationship between oscillatory power and statistical learning at electrode F8. Panel B shows a time-frequency correlation plot (Spearman's ρ) between oscillatory power and overall accuracy on the 2AFC task. In this panel, lighter colours (yellow) indicate positive correlations (Spearman's ρ) between accuracy and oscillatory power, while darker colours (blue) indicate negative correlations. Red contour lines indicate clusters of significant correlations. Panel A shows a scatterplot summarising the relationship at the ~200 msec cluster. Panel C shows the distribution of Spearman's ρ values across the scalp for the significant cluster. **$p < .001$

68% of trials ($M = .68$, $SD = .15$, Range: .31–.94), a performance level that was significantly above chance [$t(54) = 9.348$, $p < .001$, Cohen's $d = 1.261$]. Permutation testing identified two significant clusters of correlations at electrode AF4 ($p = .024$ and $p = .040$), and one cluster at electrode F8 ($p = .044$). All other electrode-level correlations were non-significant (see Supplementary Fig. S7 for full topographic results).

Electrode AF4. Fig. 8 summarises the correlation between oscillatory power and 2AFC task accuracy at electrode AF4. At this site, two significant clusters were observed (Panel B of Fig. 8). The first cluster, occurring when the first syllable was presented (~250 msec after nonword onset) and spanning 12–27 Hz, showed a positive correlation between beta power and task accuracy. The average correlation for this cluster was $\rho = .455$ ($p < .001$), indicating children with higher power in this time window and frequency, obtained higher accuracy scores (Panel A of Fig. 8, left scatterplot). The second cluster emerged after the third syllable was presented (~800 msec after nonword onset), comprising a frequency range of 14–23 Hz. At this cluster, a negative correlation between power and task accuracy was observed. The average correlation for this cluster was $\rho = -.454$ ($p < .001$), indicating that children with higher accuracy tended to show lower beta power at this time point (Panel B of Figure, right scatterplot). The spatial distribution of correlation coefficients, presented in Panel C of Fig. 8, revealed both effects were most prominent over right prefrontal regions.

Electrode F8. Fig. 9 displays results from electrode F8, where a single significant cluster of positive correlations was observed when the first syllable was presented (~200 msec after nonword onset). The frequency range of this cluster spanned 23–35 Hz. The average correlation at this cluster was $\rho = .537$ ($p < .001$) and is presented in Panel A of Fig. 9. The topographic plot, presented in Figure C of Panel 9, shows this effect was highly localised to right prefrontal scalp regions.

7. Discussion

This study examined oscillatory activity associated with auditory statistical learning in children aged 8–12 years. Statistical learning modulated beta-band power in a manner largely consistent with predictions; syllables with higher transitional probabilities were associated with greater beta desynchronisation (i.e., reduced beta power). This effect was exposure-dependent, with significant differences between the first and third syllables emerging after 100 exposures to the nonwords. Also, beta modulation was limited to left prefrontal electrodes, suggesting recruitment of language-related cortical regions during learning (Hanslmayr et al., 2011; Herfurth et al., 2022). The analyses testing an association between oscillatory power and the offline measure of statistical

learning also aligned with expectations. As predicted, lower beta power at the highly predictable third syllable was associated with better performance on an offline recognition task. Additionally, participants who failed to show increased beta at the less predictable first syllable, tended to perform more poorly. Interestingly, these effects were confined to right-prefrontal electrodes, rather than the left-lateralised sites where learning-related activity was observed. Finally, additional power modulations were observed in the theta-alpha and delta-theta bands, indicating that statistical learning engages a broader network of oscillatory processes.

7.1. Beta oscillations and auditory statistical learning in children

To our knowledge, this is the first study to demonstrate that beta oscillations are sensitive to auditory statistical learning in either and adult or paediatric sample. However, these findings align with research examining statistical learning in other modalities. In both adults and children, exposure-dependent reductions in beta power have been reported during the perception of predictable motor and visual sequences compared to random input (Bogaerts et al., 2020; Lum et al., 2024, 2025). Extending the model proposed by Engel and Fries (2010), beta desynchronisation may enable incoming sensory input to update functional networks, thereby supporting the bottom-up discovery of embedded regularities. This interpretation aligns our findings with several influential models of statistical learning (Foerde et al., 2006; Janacsek et al., 2012; Park et al., 2022; Smalle et al., 2021). An alternative possibility is that beta modulations may reflect segmentation processes, specifically the prediction of chunk onsets once the stream is perceived as concatenated pseudo-words, rather than syllable-level transitional probabilities (Benjamin et al., 2023; Fujioka et al., 2012).

Interestingly, the topographical distribution of beta modulations appears to differ by modality: motor learning effects are observed over motor areas (Lum et al., 2024, 2025), visual learning over central-parietal areas (Bogaerts et al., 2020), and, as shown here, auditory-verbal learning over left prefrontal areas. This pattern of results raises the possibility that beta desynchronisation reflects a domain-general mechanism for statistical learning (e.g., Frost et al., 2015), with its cortical distribution shaped by the neural systems specialised for processing the relevant input stream.

An important caveat to the interpretation above is the correlational nature of the present findings. The power modulations observed in this study may reflect a neural correlate or downstream consequence of learning, rather than the mechanism by which learning occurs (Bogaerts et al., 2020). Future research will therefore be needed to determine whether beta oscillations play a causal role in statistical learning. Neurofeedback paradigms, which have been successfully implemented in children, may offer a useful approach (for reviews see Enriquez-Geppert et al., 2017; Marzbani et al., 2016). The use of non-invasive brain stimulation may also be informative, particularly techniques such as transcranial alternating current stimulation (tACS), which can entrain neural activity at specific frequencies (Helfrich et al., 2014). If beta oscillations are functionally involved in statistical learning, then modulating their expression through neurofeedback or perturbation should systematically alter learning outcomes, either enhancing or impairing sensitivity to statistical regularities depending on the direction of modulation.

The current study also provides evidence that beta oscillations may be linked to processes beyond the real-time tracking of statistical structure. Correlation analyses revealed a relationship between beta activity during exposure and subsequent recognition of the nonwords. Specifically, greater beta synchronisation around the first syllable was associated with better recognition of trained items, while greater desynchronisation around the third syllable also predicted improved performance. These effects were observed at right-prefrontal electrodes. Beta synchronisation at right prefrontal sites has previously been implicated in the maintenance of task-relevant cognitive states, whereas desynchronisation has been linked to cognitive shifts and the updating of working memory representations (Schmidt et al., 2019; Wagner et al., 2018). In the context of our study, synchronisation at the start of the nonword may help suppress interference from the preceding sequence, stabilising the input stream for efficient encoding. Subsequent desynchronisation may reflect a shift toward updating or consolidating the full syllable sequence in memory. Thus, it may be the dynamic modulation of beta activity across the syllable sequence, rather than absolute power at any one position, that supports statistical learning.

7.2. The role of theta-alpha & theta-delta oscillations in auditory statistical learning

Beyond beta-band activity, our analyses revealed that statistical learning also modulated power in the theta–alpha and delta–theta frequency ranges. As with beta oscillations, it remains unclear whether these power modulations are fundamental to the learning process or correlates. Accordingly, our interpretations of their functional significance are necessarily tentative. Oscillatory power in the theta–alpha band increased bilaterally at frontal electrodes from the first to the second syllable, with no further increase from the second to the third. This effect emerged only after 100 exposures to the nonword stream, suggesting it may be related to the detection of transitional probabilities. Increases in alpha power have been associated with inhibitory effects on cortical excitability, often interpreted as protecting working memory representations by suppressing task-irrelevant stimuli (Bonnefond & Jensen, 2012; Klimesch et al., 2007). In contrast, frontal theta activity is commonly linked to the encoding of new information and the generation of predictions about forthcoming input (Clements et al., 2021; Riddle et al., 2020). Taken together, the observed increase in theta–alpha power from the first to the second syllable may reflect engagement of top-down control processes once predictable information becomes available. However, because theta–alpha activity has not previously been linked to statistical learning in this way, future research is needed to better understand its precise role.

The delta–theta Meyer, 2018). Increases in delta–theta power is also typically observed when speech is degraded or

unfamiliar, reflecting effortful integration of prosodic and syllabic information (Biau & Kotz, 2018; Mai & Wang, 2023). In the present study, the early modulation of delta–theta power might reflect children's rapid extraction of transitional probability information, consistent with the idea that delta–theta oscillations support the initial stages of statistical learning by tracking syllable-level regularities. Since this effect emerged within 100 exposures but was absent later, suggests that delta–theta activity contributes most strongly at the earliest stages of learning, when children are first detecting regularities in the stream.

7.3. *Future research*

This study suggests that in children, statistical learning is associated with topographically specific modulations in delta, theta, alpha, and beta band power. However, it remains unclear whether these effects extend to younger children or infants. Although robust statistical learning has been observed in infancy (e.g., Saffran, Aslin, & Newport, 1996; Saffran & Wilson, 2003), oscillatory activity across frequency bands continues to mature throughout early development (e.g., Gasser et al., 1988; Rodríguez-Martínez et al., 2015). For example, a consistent finding in developmental EEG studies is that power in all frequency bands decreases with age, likely reflecting synaptic pruning and the emergence of more efficient, specialised functional networks (Whitford et al., 2007). These changes are accompanied by shifts in relative spectral power, with slower rhythms (delta, theta) dominating early childhood and faster rhythms (beta, gamma) becoming more prominent over time (Clarke et al., 2001). How these maturational changes affect statistical learning remains an open question. Some studies have reported superior statistical learning in children relative to adults, at least as measured via a response-based pattern learning task (Janacsek et al., 2012), raising the possibility that a cortex dominated by slower oscillations may confer a statistical learning advantage. However, given that such findings have not been replicated in the language domain (Moreau, 2022; Saffran et al., 1997), it is also possible that the oscillatory mechanisms supporting statistical learning reach functional maturity relatively early. To resolve this, future research will need to examine oscillatory dynamics of statistical learning across a broader developmental window, and across different domains and modalities.

8. Conclusion

This study provides new evidence linking beta-band oscillatory activity to auditory statistical learning in older children. Specifically, we show that beta desynchronisation is sensitive to predictable syllabic co-occurrences within continuous speech. Notably, this desynchronisation peaked at the third syllable, suggesting that beta oscillations may support the integration of sequential syllables into stable nonword representations. The left-lateralised distribution of beta activity further implies that auditory statistical learning in this age group may recruit language-related cortical regions. In addition, we observed modulation of theta-alpha and delta-theta power, suggesting that multiple oscillatory systems may contribute to auditory statistical learning.

CRediT authorship contribution statement

Jarrad A.G. Lum: Writing – review & editing, Writing – original draft, Formal analysis, Conceptualization. **Christine N. Moreau:** Writing – review & editing, Supervision, Resources, Project administration, Methodology, Investigation, Data curation, Conceptualization. **Li-Ann Leow:** Writing – review & editing. **Welber Marinovic:** Writing – review & editing. **Sarah J. Lum:** Writing – review & editing. **Marc F. Joanisse:** Writing – review & editing, Supervision, Resources, Project administration, Methodology, Investigation, Funding acquisition, Data curation, Conceptualization. **Laura J. Batterink:** Writing – review & editing, Writing – original draft, Supervision, Resources, Project administration, Methodology, Investigation, Funding acquisition, Data curation, Conceptualization.

Acknowledgements

This research was supported by Natural Sciences and Engineering Research Council of Canada Discovery Grants to LJB and MFJ. We would like to thank Krystal Flemming, Kailee Liesemer, Jessica Lammert, and Isabel Child for help with testing the participants. Thanks also to Dr. Nicolette Armstrong for her input at the beginning of this project and later with EEG testing. We would also like to extend our appreciation to children and adults for participating in this study.

Scientific transparency statement

DATA: All raw and processed data supporting this research are publicly available: https://data.mendeley.com/datasets/3rmh27h4y5/2, https://osf.io/e3ajh.
CODE: All analysis code supporting this research is publicly available: https://osf.io/e3ajh.
MATERIALS: All study materials supporting this research are publicly available: https://data.mendeley.com/datasets/3rmh27h4y5/2.
DESIGN: This article reports, for all studies, how the author(s) determined all sample sizes, all data exclusions, all data inclusion and exclusion criteria, and whether inclusion and exclusion criteria were established prior to data analysis.
PRE-REGISTRATION: No part of the study procedures was pre-registered in a time-stamped, institutional registry prior to the research being conducted. No part of the analysis plans was pre-registered in a time-stamped, institutional registry prior to the research being conducted.
For full details, see the *Scientific Transparency Report* in the supplementary data to the online version of this article.

Supplementary data

Supplementary data to this article can be found online at https://doi.org/10.1016/j.cortex.2025.11.003.

REFERENCES

Aslin, R. N. (2017). Statistical learning: A powerful mechanism that operates by mere exposure. *Wiley Interdisciplinary Reviews: Cognitive Science, 8*(1–2) e1373. https://doi.org/10.1002/wcs.1373

Bailey, N., Biabani, M., Hill, A., Miljevic, A., Rogasch, N., McQueen, B., Murphy, O., & Fitzgerald, P. (2023). Introducing RELAX: An automated pre-processing pipeline for cleaning EEG data-part 1: Algorithm and application to oscillations. *Clinical Neurophysiology, 149*, 178–201. https://doi.org/10.1016/j.clinph.2023.01.017

Bailey, N., Hill, A., Biabani, M., Murphy, O., Rogasch, N., McQueen, B., Miljevic, A., & Fitzgerald, P. (2023). RELAX part 2: A fully automated EEG data cleaning algorithm that is applicable to event-related-potentials. *Clinical Neurophysiology, 149*, 202–222. https://doi.org/10.1016/j.clinph.2023.01.018

Batterink, L. J. (2017). Rapid statistical learning supporting word extraction from continuous speech. *Psychological Science, 28*(7), 921–928. https://doi.org/10.1177/0956797617698226

Batterink, L. J., & Paller, K. A. (2017). Online neural monitoring of statistical learning. *Cortex; A Journal Devoted to the Study of the Nervous System and Behavior, 90*, 31–45. https://doi.org/10.1016/j.cortex.2017.02.004

Batterink, L. J., Paller, K. A., & Reber, P. J. (2019). Understanding the neural bases of implicit and statistical learning. *Topics in Cognitive Science, 11*(3), 482–503. https://doi.org/10.1111/tops.12420

Benjamin, L., Fló, A., Palu, M., Naik, S., Melloni, L., & Dehaene-Lambertz, G. (2023). Tracking transitional probabilities and segmenting auditory sequences are dissociable processes in adults and neonates. *Developmental Science, 26*(2) e13300. https://doi.org/10.1111/desc.13300

Benjamini, Y., & Hochberg, Y. (1995). Controlling the false discovery rate: A practical and powerful approach to multiple testing. *Journal of the Royal Statistical society: Series B (Methodological), 57*(1), 289–300. https://doi.org/10.1111/j.2517-6161.1995.tb02031.x

Berger, S., & Batterink, L. J. (2024). Children extract a new linguistic rule more quickly than adults. *Developmental Science, 27*(4) e13498. https://doi.org/10.1111/desc.13498

Biau, E., & Kotz, S. A. (2018). Lower beta: A central coordinator of temporal prediction in multimodal speech. *Frontiers in Human Neuroscience, 12*, 434. https://doi.org/10.3389/fnhum.2018.00434.

Bigdely-Shamlo, N., Mullen, T., Kothe, C., Su, K.-M., & Robbins, K. A. (2015). The PREP pipeline: Standardized preprocessing for large-scale EEG analysis. *Frontiers in Neuroinformatics, 9*(6), 16. https://doi.org/10.3389/fninf.2015.00016

Bishop, D. V. M. (2003). In *Test for Reception of Grammar (TROG-2)* (2nd ed.). Harcourt Assessment.

Bogaerts, L., Richter, C. G., Landau, A. N., & Frost, R. (2020). Beta-band activity is a signature of statistical learning. *Journal of Neuroscience, 40*(39), 7523–7530. https://doi.org/10.1523/JNEUROSCI.0771-20.2020

Bonnefond, M., & Jensen, O. (2012). Alpha oscillations serve to protect working memory maintenance against anticipated distracters. *Current Biology, 22*(20), 1969–1974. https://doi.org/10.1016/j.neulet.2009.11.028

Buzsaki, G., & Draguhn, A. (2004). Neuronal oscillations in cortical networks. *Science, 304*(5679), 1926–1929. https://doi.org/10.1126/science.1099745

Castellanos, N. P., & Makarov, V. A. (2006). Recovering EEG brain signals: Artifact suppression with wavelet enhanced independent component analysis. *Journal of Neuroscience Methods, 158*(2), 300–312. https://doi.org/10.1016/j.jneumeth.2006.05.033

Chang, A., Bosnyak, D. J., & Trainor, L. J. (2018). Beta oscillatory power modulation reflects the predictability of pitch change. *Cortex; A Journal Devoted to the Study of the Nervous System and Behavior, 106*, 248–260. https://doi.org/10.1016/j.cortex.2018.06.008

Clarke, A. R., Barry, R. J., McCarthy, R., & Selikowitz, M. (2001). Age and sex effects in the EEG: Development of the normal child. *Clinical Neurophysiology, 112*(5), 806–814. https://doi.org/10.1016/S1388-2457(01)00488-6

Clements, G. M., Bowie, D. C., Gyurkovics, M., Low, K. A., Fabiani, M., & Gratton, G. (2021). Spontaneous alpha and theta oscillations are related to complementary aspects of cognitive control in younger and older adults. *Frontiers in Human Neuroscience, 15* 621620. https://doi.org/10.3389/fnhum.2021.621620

Cohen, M. X. (2014). *Analyzing neural time series data: Theory and practice*. MIT press.

Cohen, M. X. (2017). Where does EEG come from and what does it mean? *Trends in Neurosciences, 40*(4), 208–218. https://doi.org/10.1016/j.tins.2017.02.004

Delorme, A., & Makeig, S. (2004). EEGLAB: An open source toolbox for analysis of single-trial EEG dynamics including independent component analysis. *Journal of Neuroscience Methods, 134*(1), 9–21. https://doi.org/10.1016/j.jneumeth.2003.10.009

Engel, A. K., & Fries, P. (2010). Beta-band oscillations—signalling the status quo? *Current Opinion in Neurobiology, 20*(2), 156–165. https://doi.org/10.1016/j.conb.2010.02.015

Enriquez-Geppert, S., Huster, R. J., & Herrmann, C. S. (2017). EEG-neurofeedback as a tool to modulate cognition and behavior: A review tutorial. *Frontiers in Human Neuroscience, 11*, 51. https://doi.org/10.3389/fnhum.2017.00051

Fan, T., Decker, W., & Schneider, J. (2024). The domain-specific neural basis of auditory statistical learning in 5–7-year-old children. *Neurobiology of Language, 5*(4), 981–1007. https://doi.org/10.1162/nol_a_00156

Finn, A. S., Kharitonova, M., Holtby, N., & Sheridan, M. A. (2019). Prefrontal and hippocampal structure predict statistical learning ability in early childhood. *Journal of Cognitive Neuroscience, 31*(1), 126–137. https://doi.org/10.1162/jocn_a_01342

Foerde, K., Knowlton, B. J., & Poldrack, R. A. (2006). Modulation of competing memory systems by distraction. *Proceedings of the National Academy of Sciences, 103*(31), 11778–11783. https://doi.org/10.1073/pnas.0602659103

Frost, R., Armstrong, B. C., Siegelman, N., & Christiansen, M. H. (2015). Domain generality versus modality specificity: The paradox of statistical learning. *Trends in Cognitive Sciences, 19*(3), 117–125. https://doi.org/10.1016/j.tics.2014.12.010

Fujioka, T., Trainor, L. J., Large, E. W., & Ross, B. (2012). Internalized timing of isochronous sounds is represented in neuromagnetic beta oscillations. *Journal of Neuroscience, 32*(5), 1791–1802. https://doi.org/10.1523/JNEUROSCI.4107-11.2012

Gómez, R. L., & Gerken, L. (2000). Infant artificial language learning and language acquisition. *Trends in Cognitive Sciences, 4*(5), 178–186. https://doi.org/10.1016/S1364-6613(00)01467-4

Gasser, T., Verleger, R., Bächer, P., & Sroka, L. (1988). Development of the EEG of school-age children and adolescents. I. Analysis of band power. *Electroencephalography and Clinical Neurophysiology, 69*(2), 91–99.

Hanslmayr, S., Volberg, G., Wimber, M., Raabe, M., Greenlee, M. W., & Bäuml, K.-H. T. (2011). The relationship between brain oscillations and BOLD signal during memory formation: A combined EEG–fMRI study. *Journal of Neuroscience, 31*(44), 15674–15680. https://doi.org/10.1523/JNEUROSCI.3140-11.2011

Helfrich, R. F., Schneider, T. R., Rach, S., Trautmann-Lengsfeld, S. A., Engel, A. K., & Herrmann, C. S. (2014). Entrainment of brain oscillations by transcranial alternating

current stimulation. *Current Biology, 24*(3), 333–339. https://doi.org/10.1016/j.cub.2013.12.041

Herfurth, K., Harpaz, Y., Roesch, J., Mueller, N., Walther, K., Kaltenhaeuser, M., Pauli, E., Goldstein, A., Hamer, H., & Buchfelder, M. (2022). Localization of beta power decrease as measure for lateralization in pre-surgical language mapping with magnetoencephalography, compared with functional magnetic resonance imaging and validated by Wada test. *Frontiers in Human Neuroscience, 16* 996989. https://doi.org/10.3389/fnhum.2022.996989

Isbilen, E. S., & Christiansen, M. H. (2022). Statistical learning of language: A meta-analysis into 25 years of research. *Cognitive Science, 46*(9) e13198. https://doi.org/10.1111/cogs.13198

Janacsek, K., Fiser, J., & Nemeth, D. (2012). The best time to acquire new skills: Age-related differences in implicit sequence learning across the human lifespan. *Developmental Science, 15*(4), 496–505. https://doi.org/10.1111/j.1467-7687.2012.01150.x

Kidd, E. (2012). Implicit statistical learning is directly associated with the acquisition of syntax. *Developmental Psychology, 48*(1), 171. https://doi.org/10.1037/a0025405

Klimesch, W., Sauseng, P., & Hanslmayr, S. (2007). EEG alpha oscillations: The inhibition–timing hypothesis. *Brain Research Reviews, 53*(1), 63–88. https://doi.org/10.1016/j.brainresrev.2006.06.003

Kloosterman, N. A., Meindertsma, T., Hillebrand, A., van Dijk, Lamme, V. A., & Donner, T. H. (2015). Top-down modulation in human visual cortex predicts the stability of a perceptual illusion. *Journal of Neurophysiology, 113*(4), 1063–1076. https://doi.org/10.1152/jn.00338.2014.

Kuhl, P. K., Stevens, E., Hayashi, A., Deguchi, T., Kiritani, S., & Iverson, P. (2006). Infants show a facilitation effect for native language phonetic perception between 6 and 12 months. *Developmental Science, 9*(2), F13–F21. https://doi.org/10.1111/j.1467-7687.2006.00468.x

Lum, J. A. G., Barham, M. P., Hyde, C., Hill, A. T., White, D. J., Hughes, M. E., & Clark, G. M. (2024). Top-down and bottom-up oscillatory dynamics regulate implicit visuomotor sequence learning. *Cerebral Cortex, 34*(7). https://doi.org/10.1093/cercor/bhae266

Lum, J. A. G., Hamilton, K., Leow, L. A., Marinovic, W., Fuelscher, I., Barhoun, P., Ford, T. C., Hill, A., Nahravani, S., Kirkovski, M., Enticott, P., & Hyde, C. (2025). Atypical beta oscillatory dynamics are related to poor procedural learning in children with developmental coordination disorder. *Developmental Science, 28*(4) e70031. https://doi.org/10.1111/desc.70031

Mai, G., & Wang, W. S. Y. (2023). Distinct roles of delta-and theta-band neural tracking for sharpening and predictive coding of multi-level speech features during spoken language processing. *Human Brain Mapping, 44*(17), 6149–6172. https://doi.org/10.1002/hbm.26503.

Maris, E., & Oostenveld, R. (2007). Nonparametric statistical testing of EEG-and MEG-data. *Journal of Neuroscience Methods, 164*(1), 177–190. https://doi.org/10.1016/j.jneumeth.2007.03.024

Marzbani, H., Marateb, H. R., & Mansourian, M. (2016). Neurofeedback: A comprehensive review on system design, methodology and clinical applications. *Basic and Clinical Neuroscience, 7*(2), 143–158. https://doi.org/10.15412/J.BCN.03070208

McNealy, K., Mazziotta, J. C., & Dapretto, M. (2006). Cracking the language code: Neural mechanisms underlying speech parsing. *Journal of Neuroscience, 26*(29), 7629–7639. https://doi.org/10.1523/JNEUROSCI.5501-05.2006

McNealy, K., Mazziotta, J. C., & Dapretto, M. (2010). The neural basis of speech parsing in children and adults. *Developmental Science, 13*(2), 385–406. https://doi.org/10.1111/j.1467-7687.2009.00895.x

McNealy, K., Mazziotta, J. C., & Dapretto, M. (2011). Age and experience shape developmental changes in the neural basis of language-related learning. *Developmental Science, 14*(6), 1261–1282. https://doi.org/10.1111/j.1467-7687.2011.01075.x

Meyer, L. (2018). The neural oscillations of speech processing and language comprehension: state of the art and emerging mechanisms. *European Journal of Neuroscience, 48*(7), 2609–2621. https://doi.org/10.1111/ejn.13748.

Moreau, C. N. (2022). *Statistical learning in children and adults: Evidence from behavioural and neural entrainment data*. Mendeley. https://doi.org/10.17632/3RMH27H4Y5.2

Moreau, C. N., Joanisse, M. F., Mulgrew, J., & Batterink, L. J. (2022). No statistical learning advantage in children over adults: Evidence from behaviour and neural entrainment. *Developmental Cognitive Neuroscience, 57* 101154. https://doi.org/10.1016/j.dcn.2022.101154

Musall, S., Von Pföstl, V., Rauch, A., Logothetis, N. K., & Whittingstall, K. (2014). Effects of neural synchrony on surface EEG. *Cerebral Cortex, 24*(4), 1045–1053. https://doi.org/10.1093/cercor/bhs389

Nichols, T. E., & Holmes, A. P. (2002). Nonparametric permutation tests for functional neuroimaging: A primer with examples. *Human Brain Mapping, 15*(1), 1–25. https://doi.org/10.1002/hbm.1058

Park, J., Janacsek, K., Nemeth, D., & Jeon, H.-A. (2022). Reduced functional connectivity supports statistical learning of temporally distributed regularities. *Neuroimage, 260* 119459. https://doi.org/10.1016/j.neuroimage.2022.119459

Pernet, C. R., Latinus, M., Nichols, T. E., & Rousselet, G. A. (2015). Cluster-based computational methods for mass univariate analyses of event-related brain potentials/fields: A simulation study. *Journal of Neuroscience Methods, 250*, 85–93. https://doi.org/10.1016/j.jneumeth.2014.08.003

Pfurtscheller, G. (1992). Event-related synchronization (ERS): An electrophysiological correlate of cortical areas at rest. *Electroencephalography and Clinical Neurophysiology, 83*(1), 62–69. https://doi.org/10.1016/0013-4694(92)90133-3

Pfurtscheller, G., & Aranibar, A. (1977). Event-related cortical desynchronization detected by power measurements of scalp EEG. *Electroencephalography and Clinical Neurophysiology, 42*(6), 817–826. https://doi.org/10.1016/0013-4694(77)90235-8

Pfurtscheller, G., Graimann, B., Huggins, J. E., Levine, S. P., & Schuh, L. A. (2003). Spatiotemporal patterns of beta desynchronization and gamma synchronization in corticographic data during self-paced movement. *Clinical Neurophysiology, 114*(7), 1226–1236. https://doi.org/10.1016/S1388-2457(03)00067-1

Pfurtscheller, G., & Lopes da Silva, F. H. (1999). Event-related EEG/MEG synchronization and desynchronization: Basic principles. *Clinical Neurophysiology, 110*(11), 1842–1857. https://doi.org/10.1016/S1388-2457(99)00141-8

Pion-Tonachini, L., Kreutz-Delgado, K., & Makeig, S. (2019). ICLabel: An automated electroencephalographic independent component classifier, dataset, and website. *Neuroimage, 198*, 181–197. https://doi.org/10.1016/j.neuroimage.2019.05.026

Raviv, L., & Arnon, I. (2018). The developmental trajectory of children's auditory and visual statistical learning abilities: Modality-based differences in the effect of age. *Developmental Science, 21*(4) e12593. https://doi.org/10.1111/desc.12593

Ren, J., Wang, M., & Arciuli, J. (2023). A meta-analysis on the correlations between statistical learning, language, and reading outcomes. *Developmental Psychology, 59*(9), 1626. https://doi.org/10.1037/dev0001577

Riddle, J., Scimeca, J. M., Cellier, D., Dhanani, S., & D'Esposito, M. (2020). Causal evidence for a role of theta and alpha

oscillations in the control of working memory. *Current Biology, 30*(9), 1748–1754. https://doi.org/10.1016/j.cub.2020.02.065

Rodríguez-Martínez, E. I., Barriga-Paulino, C. I., Rojas-Benjumea, M. A., & Gómez, C. M. (2015). Co-Maturation of theta and low-beta rhythms during child development. *Brain Topography, 28*(2), 250–260. https://doi.org/10.1007/s10548-014-0369-3

Romberg, A. R., & Saffran, J. R. (2010). Statistical learning and language acquisition. *Wiley Interdisciplinary Reviews: Cognitive Science, 1*(6), 906–914. https://doi.org/10.1002/wcs.78

Saffran, J. R., Aslin, R. N., & Newport, E. L. (1996). Statistical learning by 8-month-old infants. *Science, 274*(5294), 1926–1928. https://10.1126/science.274.5294.192.

Saffran, J. R., Newport, E. L., & Aslin, R. N. (1996). Word segmentation: The role of distributional cues. *Journal of Memory and Language, 35*(4), 606–621. https://doi.org/10.1006/jmla.1996.0032

Saffran, J. R., Newport, E. L., Aslin, R. N., Tunick, R. A., & Barrueco, S. (1997). Incidental language learning: Listening (and learning) out of the corner of your ear. *Psychological Science, 8*(2), 101–105.

Saffran, J. R., & Wilson, D. P. (2003). From syllables to syntax: Multilevel statistical learning by 12-month-old infants. *Infancy, 4*(2), 273–284. https://doi.org/10.1207/S15327078IN0402_07

Schmidt, R., Ruiz, M. H., Kilavik, B. E., Lundqvist, M., Starr, P. A., & Aron, A. R. (2019). Beta oscillations in working memory, executive control of movement and thought, and sensorimotor function. *Journal of Neuroscience, 39*(42), 8231–8238. https://doi.org/10.1523/JNEUROSCI.1163-19.2019

Smalle, E. H., Muylle, M., Duyck, W., & Szmalec, A. (2021). Less is more: Depleting cognitive resources enhances language learning abilities in adults. *Journal of Experimental Psychology: General, 150*(12), 2423–2434. https://doi.org/10.1037/xge0001058

Wagner, J., Wessel, J. R., Ghahremani, A., & Aron, A. R. (2018). Establishing a right frontal beta signature for stopping action in scalp EEG: Implications for testing inhibitory control in other task contexts. *Journal of Cognitive Neuroscience, 30*(1), 107–118. https://doi.org/10.1162/jocn_a_01183

Weiss, S., & Mueller, H. M. (2012). Too many betas do not spoil the broth": The role of beta brain oscillations in language processing. *Frontiers in Psychology, 3*, 201. https://doi.org/10.3389/fpsyg.2012.00201.

Whitford, T. J., Rennie, C. J., Grieve, S. M., Clark, C. R., Gordon, E., & Williams, L. M. (2007). Brain maturation in adolescence: Concurrent changes in neuroanatomy and neurophysiology. *Human Brain Mapping, 28*(3), 228–237. https://doi.org/10.1002/hbm.20273.

Wonnacott, E., Newport, E. L., & Tanenhaus, M. K. (2008). Acquiring and processing verb argument structure: Distributional learning in a miniature language. *Cognitive Psychology, 56*(3), 165–209. https://doi.org/10.1016/j.cogpsych.2007.04.002